Human Molecular Genetics, 2004, Vol. 13, No. 24 **3045–3056**
doi:10.1093/hmg/ddh339
Advance Access published on October 27, 2004

A novel mechanism in recessive nephrogenic diabetes insipidus: wild-type aquaporin-2 rescues the apical membrane expression of intracellularly retained AQP2-P262L

Fabrizio de Mattia[1,†], Paul J.M. Savelkoul[1,†], Daniel G. Bichet[2], Erik-Jan Kamsteeg[1], Irene B.M. Konings[1], Nannette Marr[1], Marie-Françoise Arthus[2], Michèle Lonergan[2], Carel H. van Os[1], Peter van der Sluijs[3], Gary Robertson[4] and Peter M.T. Deen[1,*]

[1]Department of Physiology, Radboud University of Nijmegen Medical Center, Nijmegen, The Netherlands, [2]Department of Medicine, University of Montreal and Centre de Recherches, Hôpital du Sacre-Coeur de Montreal, Montreal, Quebec, Canada, [3]Department of Cell Biology, University Medical Center Utrecht, Utrecht, The Netherlands and [4]Feinberg School of Medicine of Northwestern University, Chicago, IL, USA

Received June 14, 2004; Revised and Accepted October 19, 2004

Vasopressin regulates water homeostasis through insertion of homotetrameric aquaporin-2 (AQP2) water channels in the apical plasma membrane of renal cells. *AQP2* mutations cause recessive and dominant nephrogenic diabetes insipidus (NDI), a disease in which the kidney is unable to concentrate urine in response to vasopressin. Until now, all AQP2 mutants in recessive NDI were shown to be misfolded, retained in the endoplasmic reticulum (ER) and unable to interact with wild-type (wt)-AQP2, whereas AQP2 mutants in dominant NDI are properly folded and interact with wt-AQP2, but, due to the mutation, cause missorting of the wt-AQP2/mutant complex. Here, patients of two families with recessive NDI appeared compound heterozygotes for AQP2-A190T or AQP2-R187C mutants, together with AQP2-P262L. As mutations in the AQP2 C-tail, where P262 resides, usually cause dominant NDI, the underlying cell-biological mechanism was investigated. Upon expression in oocytes, AQP2-P262L was a properly folded and functional aquaporin in contrast to the classical mutants, AQP2-R187C and AQP2-A190T. Expressed in polarized cells, AQP2-P262L was retained in intracellular vesicles and did not localize to the ER. Upon co-expression, however, AQP2-P262L interacted with wt-AQP2, but not with AQP2-R187C, resulting in a rescued apical membrane expression of AQP2-P262L. In conclusion, our study reveals a novel cellular phenotype in recessive NDI in that AQP2-P262L acts as a mutant in dominant NDI, except for that its missorting is overruled by apical sorting of wt-AQP2. Also, it demonstrates for the first time that the recessive inheritance of a disease involving a channel can be due to two cell-biological mechanisms.

INTRODUCTION

In the renal proximal tubule epithelium and descending limbs of Henle, aquaporin-1 (AQP1) is expressed in both apical and basolateral membranes enabling an optimal water reabsorption due to a parallel sodium uptake across the cells. By this mechanism, ~90% of the water content from 180 l of pro-urine formed daily is constitutively reabsorbed. Water transport in collecting ducts, however, is tightly regulated by arginine vasopressin (AVP) (1,2), which binds to its G-protein coupled V2 receptor (V2R) in the basolateral membrane of its principal cells. This binding triggers a cyclic AMP (cAMP) signaling cascade which leads to protein kinase A activation and phosphorylation of aquaporin-2 (AQP2) (3).

*To whom correspondence should be addressed at: Department of Physiology, RUNMC, PO Box 9101, 6500 HB Nijmegen, The Netherlands. Tel: +31 243617347; Fax: +31 243616413; Email: p.deen@ncmls.ru.nl
†The authors wish it to be known that, in their opinion, the first two authors should be regarded as joint First Authors.

Consequently, AQP2 is redistributed from intracellular vesicles to the apical membrane, initiating a transcellular influx of water that can exit the cells to the interstitium via AQP3 and AQP4, both present in the basolateral membrane. Conversely, withdrawal of AVP reverses this process, thereby terminating water reabsorption.

In congenital nephrogenic diabetes insipidus (NDI), a disease in which the kidney is unresponsive to AVP, this mechanism is impaired, resulting in a severe loss of water. NDI is caused by mutations in the gene encoding V2R, which comprises the X-linked form (4,5), or in *AQP2* (OMIM *107777), which results in the autosomal recessive and dominant forms of NDI (6–8).

As found in several other recessive traits, AQP2 mutants encoded in recessive NDI can be functional or not, but are all retained in the endoplasmic reticulum (ER), which is due to misfolding and consequent retention by the ER quality control (9–11). Also, the resulting mutants do not interact with wt-AQP2, which is consistent with the recessive form of inheritance of NDI. Interestingly, all AQP2 mutations in recessive NDI are found in between the first and the last (sixth) transmembrane domain, which is thought to form the water pore (12,13).

In contrast to those mentioned earlier, AQP2 mutants in dominant NDI are functional water channels, but are sorted to other subcellular organelles than wild-type (wt)-AQP2 (8,14–16). As AQP2 is expressed as a homotetramer and these AQP2 mutants are properly folded in the ER, they form heterotetramers with wt-AQP2 and missort the wt/mutant AQP2 complexes (17). The resulting lack of sufficient levels of wt-AQP2 in the apical membrane of collecting duct cells provides an explanation for dominant NDI. In contrast to mutants in recessive NDI, AQP2 mutations found in dominant NDI are all located in the C-terminal tail (Fig. 1C) and underscore the importance of this part of the protein in AQP2 sorting.

In this study, we present two families in which NDI was inherited in an autosomal recessive mode. Surprisingly, however, genomic analysis revealed that the patients were compound heterozygotes of *AQP2* gene mutations of which one was located in the AQP2 core region, whereas the other was found in the AQP2 C-tail coding region. To unravel the cell-biological mechanism underlying the recessive nature of NDI in these families, we performed extensive functional and cell-biological analyses of the encoded AQP2 mutants in *Xenopus* oocytes and polarized epithelial cells.

RESULTS

Phenotyping of the patients

Figure 1 shows partial pedigrees of the two NDI families. The proband of family A was an 11-year-old boy with a life-long history of polyuria and polydipsia. Detailed clinical evaluation revealed that he had severe NDI. By history, DI was not present in other members of his family. The proband of family B was a 6-year-old girl also referred for a documented life-long history of polyuria and polydipsia, and a 24-h urine output of 5.0 l (336 ml/kg of body weight). Her basal urine osmolality was $<$150 mOsm/kg and did not increase after administration of a therapeutic dose of 1-desamino-8-D-arginine (dDAVP). She is the only polyuric member of a three generation family.

Genotyping of the patients

Because mutations in the sex-linked *V2R* gene are the most common cause of congenital NDI and could, based on the pedigrees, not be excluded, its sequence was determined. However, no mutation in the V2R coding sequence was found in either family. Subsequent haplotype analysis and sequence analysis of the *AQP2* gene revealed that the affected male in family A (Fig. 1) is a compound heterozygote for a 568G$>$A (*AQP2* gene entry: NM 000486) nucleotide substitution in one allele and a 785C$>$T substitution in the other allele, encoding A190T and P262L amino acid changes, respectively. The affected female in family B was also a compound heterozygote, but now for 559C$>$T and 785C$>$T nucleotide substitutions, encoding R187C and P262L transitions, respectively. DNA analysis of several healthy relatives of the patients revealed that the parents and an uncle of patient A, and the mother and cousin of patient B encoded a normal wt-AQP2 and one of the two mutant AQP2 proteins, which proved the recessive inheritance of NDI in these families. The locations of the mutations in AQP2 are indicated in its topology model (Fig. 1C). The R187C and A190T mutations are located in the E-loop of AQP2, a region in which more mutations causing recessive NDI have been found. However, the P262L mutation was found in the C-terminal tail of AQP2 in which only mutations causing dominant NDI have been found.

Functional analysis in oocytes

Next, we wanted to determine whether the identified mutations could be the cause of NDI in these families or were polymorphisms. The R187C-encoding mutation present in the proband of family B has been found in other NDI patients and has been extensively studied (10,17). This mutant is a non-functional water channel that is retained in the ER. To investigate whether the A190T and P262L mutations were fundamental to NDI, these mutations were introduced into the AQP2 cDNA sequence. Subsequently, oocytes were injected with a concentration series of cRNA encoding wt-AQP2 (0.3, 1.0, 3.0 ng), AQP2-P262L (0.3, 1.0, 3.0 ng) or AQP2-A190T (1.0, 3.0 ng).

The water permeability (P_f) of oocytes expressing AQP2-A190T was not different from non-injected control oocytes (Fig. 2A). Immunoblotting of total membranes of these oocytes revealed 27, 29 and 32 kDa bands for AQP2-A190T (Fig. 2B, TM). Similar bands have been reported for other AQP2 mutants in recessive NDI (9) and represent an AQP2 degradation product, unglycosylated AQP2 and high mannose glycosylated AQP2, respectively. Although the total expression from 3 ng AQP2-A190T cRNA was more than that from 0.3 or 1 ng wt-AQP2 cRNA (Fig. 2B, TM), no expression of AQP2-A190T was observed in the plasma membrane fraction, in contrast to those of wt-AQP2 (Fig. 2B, PM). This indicated that AQP2-A190T is severely impaired in its routing to the plasma membrane. Altogether, these results

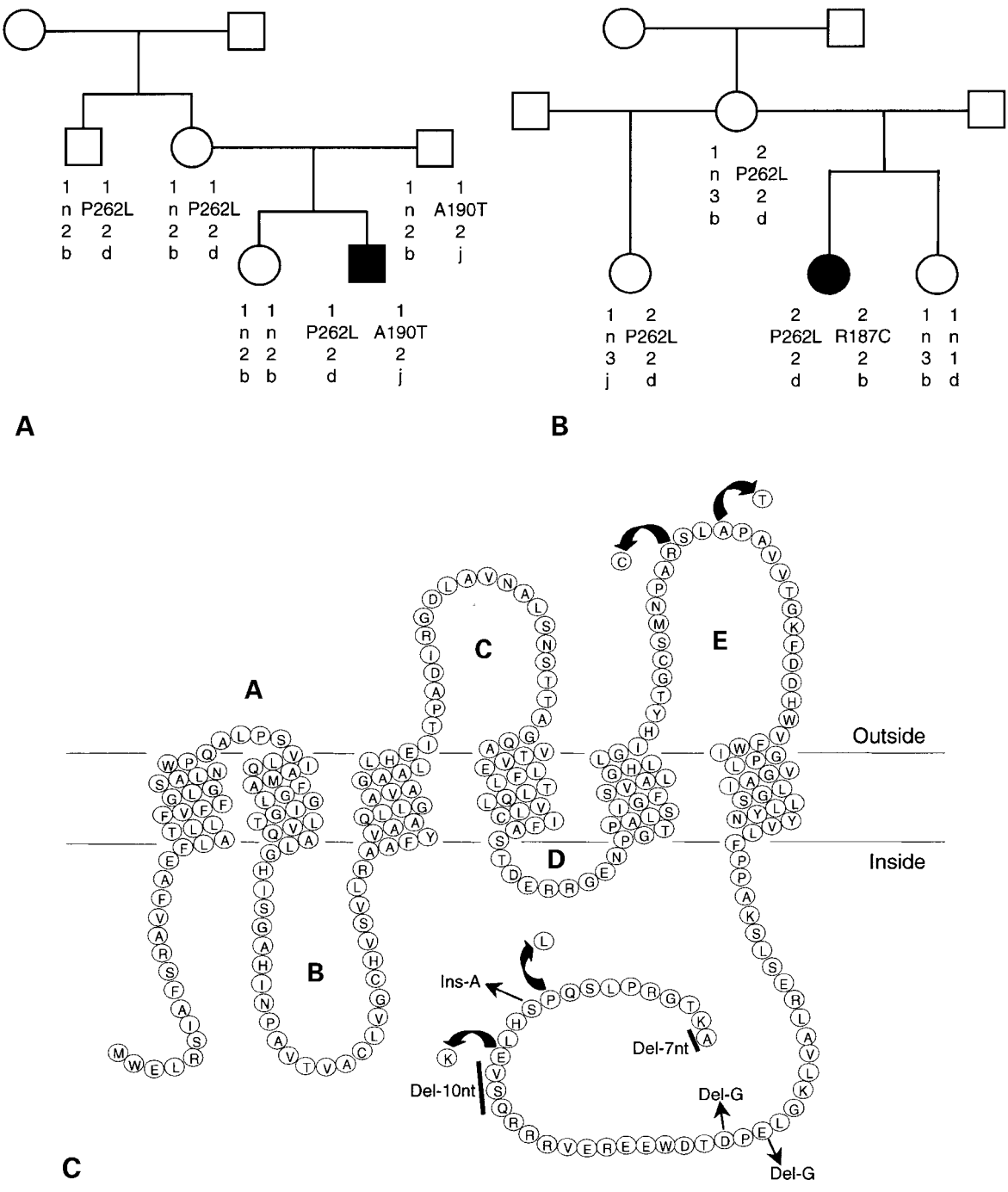

Figure 1. AQP2 mutations in the studied NDI families. (**A**, **B**) Pedigree of the two families. For the two families studied, healthy (open symbols) and affected individuals (closed symbols), and male (squares) and females (circles) are indicated. The 12q13 haplotype is represented using the marker order: centromere-AFM259vf9-*AQP2*-D12S131-AFMb007yg5-telomere (34), indicating the lengths of simple sequence tags (numbers, letters), and the AQP2 mutation (A190T, R187C or P262L) or normal (n) allele. (**C**) The localization of AQP2 mutations. The topology of AQP2 protein is predicted to consist of six transmembrane domains connected by loops A to E with the N-and C-termini located intracellularly. Loops B and E meet each other in the membrane and form the water pore. The E-loop mutations, R187C and A190T, and the C-tail mutation, P262L, give rise to the recessive NDI in the studied families. All other indicated mutations in the C-tail of AQP2 give rise to dominant NDI.

indicated that AQP2-A190T is misfolded and retained in the ER, as found for other AQP2 mutants in recessive NDI.

This was different, however, for AQP2-P262L. The P_f of oocytes expressing AQP2-P262L was higher than that of control oocytes, which indicated that AQP2-P262L is a functional water channel (Fig. 2A). Interestingly, immunoblot analysis revealed that AQP2-P262L was, besides the normal unglycosylated 29 kDa form, expressed as a 30 kDa protein, which was clearly different from the 32 kDa high mannose glycosylated AQP2 form observed for AQP2-A190T (Fig. 2B).

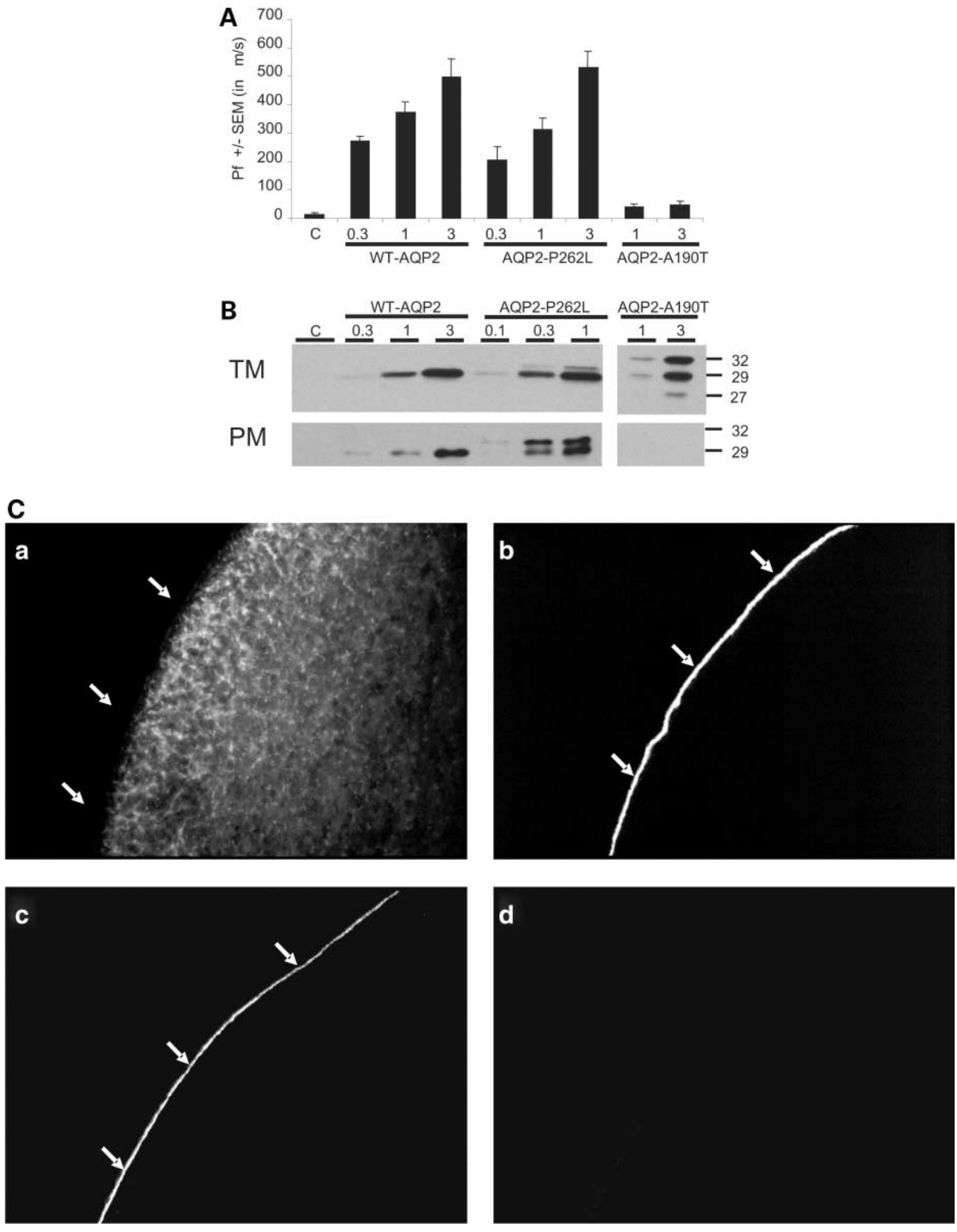

Figure 2. Expression of AQP2-P262L and AQP2-A190T in oocytes. (**A**) Water permeability in oocytes. Three days after injection of the indicated amounts of wt-AQP2, AQP2-P262L or AQP2-A190T cRNAs, oocytes were subjected to a standard swelling assay. Non-injected oocytes were taken as a control (C). Mean water permeabilities (P_f) and SEM of 10 oocytes are shown. (**B**) Expression in oocytes. From 12 oocytes injected as described earlier, total membranes (TM) or plasma membranes (PM) were isolated. Subsequently, equivalents of one oocyte were immunoblotted for AQP2. The masses in kDa of unglycosylated AQP2 (29), high mannose glycosylated AQP2 (32) and a degradation product of AQP2 (27) are indicated. (**C**) Immunocytochemistry of oocytes. Non-injected oocytes (d), or those injected with 10 ng cRNA encoding AQP2-A190T (a), or 1 ng cRNA coding for AQP2-P262L (b) or wt-AQP2 (c), were fixed at 3 days after injection and embedded in paraffin. Sections were incubated with rabbit α-AQP2 antibodies followed by Alexa488-conjugated α-rabbit antibodies. AQP2 proteins were visualized using CLSM. The plasma membranes are marked with arrows.

Comparison of the AQP2 signals in plasma membranes versus total membranes revealed that the relative plasma membrane expression of AQP2-P262L (both bands) was not less than that of wt-AQP2, which indicated that the trafficking of AQP2-P262L to the plasma membrane was not impaired.

Immunocytochemistry of oocytes

To determine the localization of AQP2-A190T and AQP2-P262L, oocytes of the same batch were subjected to immunocytochemistry. Confocal laser scanning microscopy (CLSM) revealed a dispersed staining for AQP2-A190T (Fig. 2Ca). AQP2-P262L and wt-AQP2, however, were only detected in the plasma membrane (Fig. 2Cb and c), while non-injected controls did not show any staining (Fig. 2Cd). The expression pattern of AQP2-A190T is similar to the pattern obtained for other AQP2 mutants in recessive NDI (9,11), which further indicated that AQP2-A190T is a typical ER-retained AQP2 mutant in recessive NDI. Since AQP2-R187C and AQP2-A190T are both typical AQP2 mutants in recessive NDI, AQP2-R187C was taken as a representative in following experiments.

AQP2-P262L forms heteroligomers with wt-AQP2

The ability of AQP2 mutants in dominant NDI, but not those in recessive NDI, to form heteroligomers with wt-AQP2 is fundamental to the mode of inheritance of NDI (17). Indeed, it has been shown that AQP2-R187C cannot form heteroligomers with AQP2 (17). To assess whether AQP2-P262L forms heteroligomers with AQP2 or AQP2-R187C, AQP2-P262L was co-expressed with FLAG-tagged AQP2 (F-AQP2) or AQP2-R187C (F-R187C) in oocytes. As a positive control, AQP2 was co-expressed with F-AQP2. The FLAG-tag allows specific immunoprecipitation of F-AQP2 and F-R187C and, owing to the 2 kDa mass of the FLAG-tag, discrimination of both F-AQP2 and F-R187C from AQP2-P262L on immunoblots (17). Also, the N-terminal FLAG tag does not interfere with oligomerization and plasma membrane expression of wt-AQP2 in oocytes. Two days after cRNA injections, total membranes of oocytes were isolated. After solubilization, one fraction was directly immunoblotted for AQP2 (Fig. 3, TM), while the other fraction was first subjected to anti-FLAG immunoprecipitation and then immunoblotted (Fig. 3, IP). Immunoblotting of the total membrane fractions for AQP2 revealed expression of all proteins [untagged AQP2 and AQP2-P262L of 29 kDa, F-AQP2 of 31 kDa and F-R187C of 31 (non-glycosylated) and 33 kDa (high mannose glycosylated)]. Immunoblotting of the FLAG-tag immunoprecipitates showed that AQP2-P262L and AQP2 co-precipitated with F-AQP2, but that AQP2-P262L did not co-precipitate with F-R187C (Fig. 3, IP). These data revealed that AQP2-P262L is able to form heteroligomers with wt-AQP2, but not with AQP2-R187C. Altogether, the oocyte experiments showed that AQP2-P262L is a functional water channel of 29 and 30 kDa, is expressed in the plasma membrane, heteroligomerizes with AQP2, and is not retained in the ER (based on the absence of the 32 kDa high mannose glycosylated band). Thus, if AQP2-P262L would contribute to recessive NDI in our families, it clearly showed a different cellular behavior in oocytes than other mutants in recessive NDI.

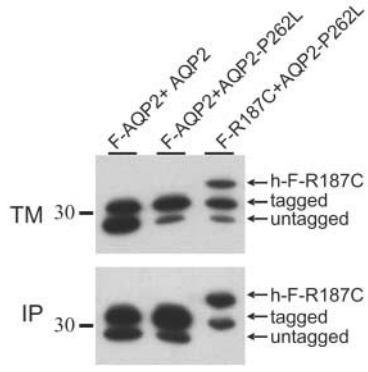

Figure 3. Heteroligomerization of AQP2-P262L in oocytes. From 30 oocytes, expressing F-AQP2 together with wt-AQP2 or AQP2-P262L, or expressing F-AQP2-R187C (F-R187C) and AQP2-P262L, total membranes (TM) were isolated, solubilized in desoxycholate and split into two fractions. One was directly immunoblotted for AQP2 (TM), whereas the other was subjected to immunoprecipitation (IP) using FLAG antibodies and then immunoblotted. Owing to the FLAG-tag, the molecular masses of F-AQP2, F-R187C and high mannose glycosylated F-R187C (h-F-R187C) are ~2 kDa higher than that of their corresponding untagged AQP2 proteins.

Localization of AQP2-P262L in polarized cells

Heterologously expressed in polarized MDCK cells, wt-AQP2 is redistributed from vesicles to the apical membrane upon stimulation with AVP or forskolin (18) and, therefore, AQP2-P262L was studied further in these cells. Following stable transfection, several MDCK cell clones expressing AQP2-P262L were grown to confluence, incubated with indomethacin (to reduce intracellular cAMP levels), treated with or without forskolin (to activate adenylate cyclase) and subjected to immunocytochemistry. CLSM analysis revealed that in unstimulated cells, AQP2-P262L mainly resides in intracellular vesicles (Fig. 4A, upper panel). Upon forskolin treatment, most AQP2-P262L remained localized in intracellular vesicles, whereas a small fraction translocated to the basolateral membrane, as shown by its partial co-localization with E-Cadherin (Fig. 4A, lower panel). wt-AQP2, which was taken along as a control, was translocated from intracellular vesicles to the apical membrane with forskolin (Fig. 4B). The vesicular and basolateral expressions of AQP2-P262L were also clearly different from the reticular pattern observed for the ER marker protein, protein disulfide isomerase (PDI) (Fig. 4C; note the complete absence of PDI from the plasma membrane). This again indicated that AQP2-P262L does not localize to the ER. AQP2-P262L also did not co-localize with the lysosome associated membrane protein 2 or the early endosome antigen 1 (data not shown), which indicated that the steady state localization of AQP2-P262L is not early or late endosomes, or lysosomes.

To test further whether the introduced leucine or the deleted proline causes AQP2-P262L retention, MDCK cells stably expressing AQP2-P262A were generated. CLSM analysis of several single clones revealed that without stimulation, AQP2-P262A is located in intracellular vesicles, while

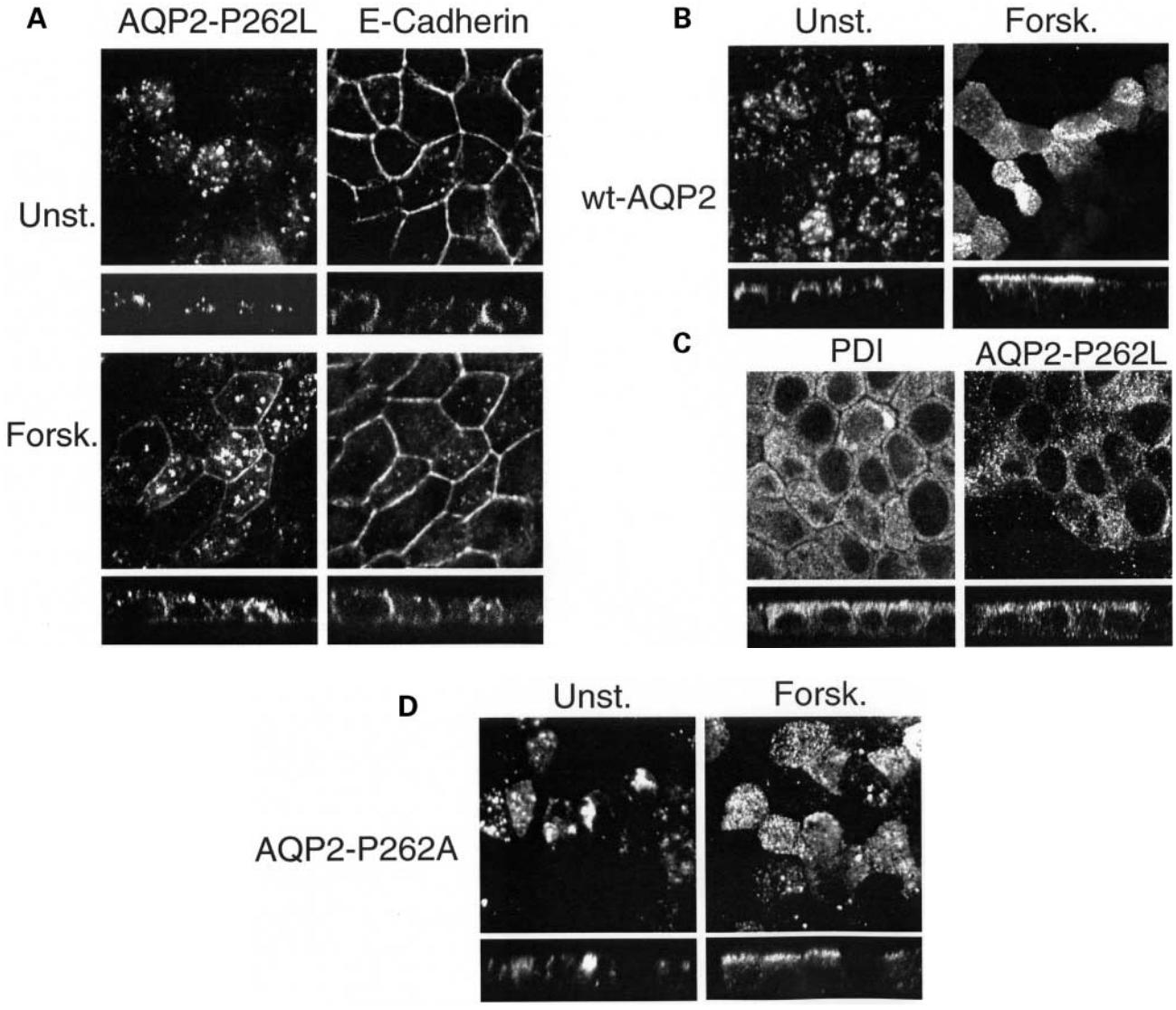

Figure 4. Localization of AQP2-P262L and AQP2-P262A in MDCK cells. MDCK cells stably expressing AQP2-P262L, AQP2-P262A or wt-AQP2 were grown to confluence on semi-permeable filters, and incubated overnight with indomethacin to reduce basal cAMP levels (unst.). To stimulate AQP2 translocation, filters were subsequently treated for 45 min with forskolin in the presence of indomethacin (forsk.). All cells were fixed, permeabilized and incubated with rabbit α-AQP2 (**A**–**D**), and rat α-E-Cadherin (A) or mouse α-PDI (C) antibodies, followed by Alexa594-conjugated anti-rabbit, Cy5-conjugated anti-rat or Alexa488-conjugated anti-mouse antibodies. CLSM X–Y and X–Z images reveal that AQP2-P262L is mainly retained in intracellular vesicles with some basolateral expression upon forskolin treatment (A). In contrast, wt-AQP2 (B) and AQP2-P262A (D) are translocated from intracellular vesicles to the apical membrane with forskolin. The expression pattern of AQP2-P262L is different from that of the ER protein PDI (C).

forskolin stimulation induced its translocation to the apical membrane (Fig. 4D). As a similar redistribution was found for wt-AQP2 (Fig. 4B), these data indicated that the retention of AQP2-P262L is due to the introduction of a leucine at position 262.

Heteroligomerization with wt-AQP2 overrules the missorting of AQP2-P262L

Missorting of wt-AQP2 upon co-expression and heteroligomerization with missorted AQP2 mutants underlies dominant NDI (14–16). As AQP2-P262L is retained in intracellular vesicles (Fig. 4) and interacts with wt-AQP2 in oocytes (Fig. 3), we wanted to determine whether the recessive trait of NDI in these families would become apparent when AQP2-P262L would be co-expressed with wt-AQP2 in MDCK cells. To discriminate AQP2-P262L and wt-AQP2, MDCK cells stably-expressing GFP-tagged wt-AQP2 (G-AQP2) were stably transfected for FLAG-tagged AQP2-P262L (F-AQP2-P262L). As we did not succeed to generate polarized cell lines stably expressing G-AQP2-R187C and F-AQP2-P262L, polarized MDCK cells stably expressing G-AQP2-R187C were transiently transfected for F-AQP2-P262L. MDCK cells stably expressing each AQP2 protein alone were taken along as references.

Immunoblot analysis of cells expressing F-AQP2-P262L alone revealed bands of 31 and 32 kDa (Fig. 5A), which is

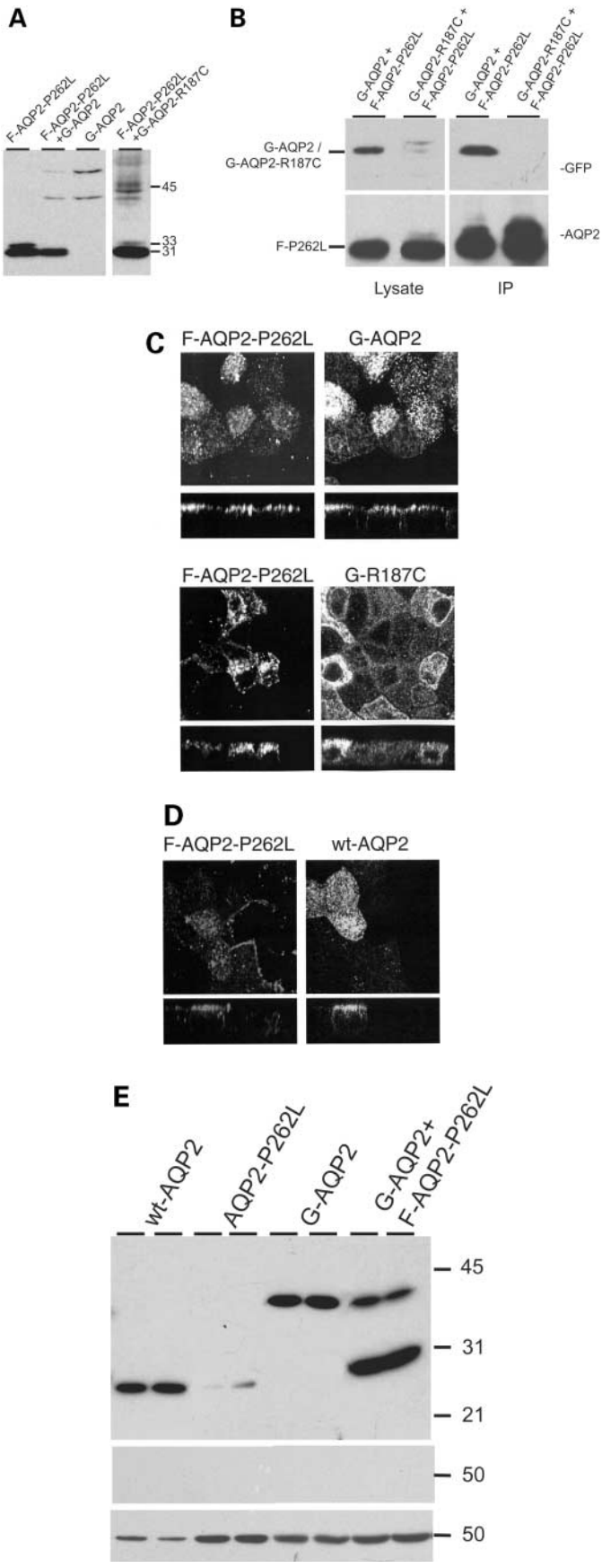

consistent with the mass of the 2 kDa FLAG-tag added to untagged AQP2-P262L of 29 and 30 kDa, respectively. G-AQP2 was expressed as 40 and 60 kDa proteins (second and third lanes), while G-AQP2-R187C (Fig. 5A, right panel) was expressed as 40 and (about) 43–46 kDa proteins. On the basis of the masses observed for the untagged forms, the 40, 43–46 and 60 kDa proteins likely represent unglycosylated, high mannose and complex glycosylated G-AQP2 proteins, respectively. Interestingly, in cell lines expressing both G-AQP2 and F-AQP2-P262L, the 32 kDa band of F-AQP2-P262L was not observed, in contrast to its 31 kDa form, whereas both F-AQP2-P262L bands were observed upon co-expression with G-AQP2-R187C.

To analyze whether F-AQP2-P262L interacts with G-AQP2 and/or G-AQP2-R187C in MDCK cells, cells co-expressing these proteins were subjected to immunoprecipitations using FLAG antibodies. Immunoblots of the lysates of these cells revealed that all three proteins were well detectable (Fig. 5B, lysate). However, immunoblot analysis of the precipitates revealed strong signals for F-AQP2-P262L and G-AQP2, but G-AQP2-R187C could not be detected. This indicated that G-AQP2, but not G-AQP2-R187C, interacts with F-AQP2-P262L in MDCK cells.

To analyze the subcellular localization of AQP2-P262L, the cells were pre-incubated with indomethacin, treated with or without forskolin and subjected to immunocytochemistry. CLSM analysis demonstrated that, independent of forskolin administration, the subcellular localization of F-AQP2-P262L was not different from that of untagged AQP2-P262L and, as reported (9), G-AQP2 was expressed in the

Figure 5. Expression of AQP2-P262L and GFP-AQP2 in MDCK cells. Native, G-AQP2 and G-AQP2-R187C expressing MDCK cells were transfected with an F-AQP2-P262L expression construct. (**A**) Immunoblot analysis. Immunoblots of transfected cells revealed 31 and 32 kDa specific bands for F-AQP2-P262L (first lane, right panel), signals of ca. 40 and 60 kDa for G-AQP2 (third lane), and 40 and ~42 kDa signals for G-AQP2-R187C (right panel). Although cells co-expressing F-AQP2-P262L and G-AQP2-R187C show both F-AQP2-P262L bands (right panel), those co-expressing F-AQP2-P262L and G-AQP2 show only the 31 kDa F-AQP2-P262L band (second lane). (**B**) Co-immunoprecipitation with F-AQP2-P262L. Cells co-expressing F-AQP2-P262L with G-AQP2 or G-AQP2-R187C were solubilized in desoxycholate, subjected to FLAG immunoprecipitation assays and immunoblotted for GFP (upper panel) or AQP2 (lower panel). Although all proteins were clearly present in the cell lysates (indicated), G-AQP2, but not G-AQP2-R187C, co-immunoprecipitated with F-AQP2-P262L. (**C, D**) Immunocytochemical analysis. MDCK cells expressing F-AQP2-P262L together with G-AQP2 or G-AQP2-R187C (G-R187C) (C) or cells expressing F-AQP2-P262L together with wt-AQP2 (D) were grown on filters and treated with forskolin as described in Figure 4. The filters were incubated with mouse α-FLAG antibodies alone (C) or combined with rabbit anti-AQP2 antibodies followed by species-specific Alexa fluorophore coupled secondary antibodies. CLSM analysis revealed that in cells expressing F-AQP2-P262L together with G-AQP2 (C) or wt-AQP2 (D), both AQP2 proteins co-localize mainly in the apical membrane, respectively. In contrast, in cells co-expressing F-AQP2-P262L and G-R187C, F-AQP2-P262L is mainly localized in intracellular vesicles and does not co-localize with G-R187C (C, lower panel). (**E**) Apical cell surface expression. Cells expressing wt-AQP2, G-AQP2 or AQP2-P262L alone, or both G-AQP2 and F-AQP2-P262L (indicated), were grown and treated with indomethacin and forskolin as described in Figure 4. Following apical cell surface biotinylation of duplicate samples, the biotinylated proteins were precipitated with streptavidin–agarose beads and immunoblotted for AQP2 (upper panel). Immunoblotting for actin revealed no signal in the biotinylation samples (middle panel), whereas strong signals were obtained in the corresponding cell lysates (lower panel).

apical membrane (data not shown). In cells co-expressing G-AQP2 and F-AQP2-P262L, however, both proteins seemed to co-localize in the apical membrane, whereas some co-staining was found in the basolateral membrane (Fig. 5C, upper panel). In contrast, in cells co-expressing F-AQP2-R187C and F-AQP2-P262L, both proteins showed a similar distribution when expressed alone (Fig. 4) and did not co-localize (Fig. 5C, lower panel). These localizations were independent of stimulation with forskolin (data not shown). As we were not able to generate MDCK cells stably expressing wt-AQP2 and F-AQP2-P262L, we transiently co-transfected both expression construct into MDCK cells and stimulated them with forskolin. Subsequent confocal analysis revealed that in the few cells that co-expressed both proteins, they co-localized mainly in the apical membrane (Fig. 5D).

To discriminate expression in the apical membrane or subapical regions of the cell, MDCK cells expressing wt-AQP2, G-AQP2 or F-AQP2-P262L only, or co-expressing G-AQP2 and F-AQP2-P262L, were stimulated with forskolin and subjected to apical cell surface biotinylation assays (Fig. 5E). Following immunoblotting, semi-quantification of the signals revealed ~5-fold less AQP2-P262L expression in the apical membrane than that of wt-AQP2 [1.3 versus 6.3 arbitrary units (AU); upper panel]. Upon co-expression with G-AQP2, however, ~10-fold more F-AQP2-P262L was expressed in the apical membrane than when expressed alone (16.6 versus 1.3 AU). For G-AQP2, co-expression with AQP2-P262L led to a slight reduction in apical membrane expression (10.9–8.0 AU). The absence of actin in the biotinylation samples (middle panel) and its presence in the corresponding cell lysates (lower panel) reveal the specificity of the biotinylation assays for proteins present in the apical membrane. These blotting data confirmed the increased expression of AQP2-P262L in the apical membrane upon co-expression with G-AQP2 and indicated that AQP2-P262L is sorted to the apical membrane upon heterotetramerization with wt-AQP2.

DISCUSSION

Analysis of the patients

In this study, haplotype and sequence analysis of the *V2R* and *AQP2* genes revealed novel mutations in two separate families with recessive NDI. The affected male in family A (Fig. 1) appeared to be a compound heterozygote for 568G>A and 785C>T substitution in the *AQP2* gene, encoding A190T and P262L mutations, respectively. The female proband of family B (Fig. 1) appeared to be a compound heterozygote for 559C>T and 785C>T *AQP2* gene mutation, coding for R187C and P262L mutations, respectively. Haplotype analysis of both families revealed that the P262L mutation co-segregated with identical lengths for the simple sequence tags D12S131 and AFMb007yg5, whereas the length of the AFM259vf9-tag differed. If a recombination event occurred between this common haplotype and the more distant locus AFM259vf9, the P262L mutation could have the same ancestry. However, we have been unable to reconstruct the family trees to that degree to demonstrate this.

AQP2-A190T and AQP2-R187C are classical AQP2 mutants in recessive NDI

Until now, all patients with recessive NDI due to *AQP2* gene mutations encode mutations found in between the first and last transmembrane domain. Although some showed a residual water transport capacity, most are non-functional (9–11) and all were retained in the ER, as concluded from their 29 (unglycosylated) and 32 kDa (high mannose glycosylated) expression forms, their dispersed 'reticular' expression pattern and their reduced stability compared with wt-AQP2 (10,19,20). As found for AQP2 mutants and many other proteins in diseases, this is likely due to misfolding, ER retention by quality control molecular chaperones and subsequent degradation via the proteasomal pathway (21–23). Presumably due to their misfolding, these AQP2 mutants are expressed as monomers and are not able to heteroligomerize and interfere with the further maturation and routing of wt-AQP2 in its pathway to the apical membrane, which is in line with the recessive nature of inheritance (17). As reported (10,16) and as shown in this study (Figs 2, 3 and 5), AQP2-R187C exerts all these characteristics. In line with a study from Kuwahara *et al.* (24), AQP2-A190T also showed the typical 29 and 32 kDa bands, was severely impaired in its trafficking to the plasma membrane and showed a dispersed staining pattern (Fig. 2). Therefore, both AQP2-R187C and AQP2-A190T can be classified as typical AQP2 mutants in recessive NDI.

The cellular phenotype of AQP2-P262L is similar to AQP2 mutants in dominant NDI

Our expression studies, however, showed a completely different cellular phenotype for AQP2-P262L when compared with classical mutants in recessive NDI. At first, the absence of the 32 kDa high mannose form (Fig. 2B), the plasma membrane expression in oocytes (Fig. 2B and C) and the lack of co-localization with an ER marker protein in MDCK cells (Fig. 4C) indicated that AQP2-P262L escaped the ER quality control and was, as such, not considered to be misfolded by the cell. Secondly, AQP2-P262L was able to assemble into heteroligomers with AQP2 (Figs 3 and 5B), which is never observed for classical AQP2 mutants in recessive NDI (17). Thirdly, in contrast to most other mutants in recessive NDI, AQP2-P262L is a functional water channel (Fig. 2). Although not corroborated by a study from Kuwahara *et al.* (24), this is in line with water permeability measurements on AQP2-P262L in yeast (25).

As such, AQP2-P262L showed a cellular phenotype clearly different from other AQP2 mutants in recessive NDI. Instead, and consistent with the molecular location of the mutation, it exerted all the characteristics that have been found for AQP2 mutants in dominant NDI (8,14–16).

Dominancy of apical sorting signals in wt-AQP2 over the retention signals of AQP2-P262L explains recessive NDI

A cell-biological explanation for its involvement in recessive instead of dominant NDI became apparent when AQP2-P262L was co-expressed with GFP-tagged or untagged AQP2 in MDCK cells (Fig. 5). Expressed on its own, most of AQP2-P262L resided in intracellular vesicles of unknown

identity, of which only a small fraction located in the basolateral (Figs 4 and 5D) and apical membrane (Fig. 5E) upon stimulation with forskolin. With forskolin stimulation, the level of apical membrane localization of AQP2-P262L was strongly reduced compared with that of wt-AQP2 (Figs 4 and 5E). Upon co-expression with G-AQP2 or untagged AQP2, however, intracellular retention of AQP2-P262L was greatly reduced (Fig. 5C–E). Instead and independent of forskolin stimulation, both proteins mainly localized in the apical membrane, whereas some were detected in the basolateral membrane (Fig. 5C and D). In contrast and in line with the recessive nature of NDI in these families, co-expression with G-AQP2-R187C did not result in apical membrane expression of F-AQP2-P262L (Fig. 5C).

Several data indicate that the localization of F-AQP2-P262L in the apical membrane is a consequence of its heteroligomerization with AQP2. At first, in oocytes and MDCK cells AQP2-P262L interacted with wt-AQP2, but not with AQP2-R187C (Figs 3 and 5B). This is in line with our findings that AQP2 assembly into tetramers occurs in the ER and that AQP2 mutants that pass the ER are multimers (14–17,26). Secondly, the apical membrane localization of F-AQP2-P262L in MDCK cells was strongly increased upon co-expression with untagged or tagged AQP2 (Fig. 5C–E), but did not with G-AQP2-R187C (Fig. 5C). As reported, G-AQP2 mainly resides in the apical membrane, independent of forskolin stimulation (9), but the rescue of apical membrane expression of F-AQP2-P262L upon co-expression with G-AQP2 or untagged AQP2 shows that the rescue is not due to the GFP-tag. In addition, co-expression of G-AQP2 with two AQP2 mutants in dominant NDI resulted in the retention of the formed G-AQP2/mutant complexes in intracellular structures (unpublished data). The slightly reduced apical membrane expression of G-AQP2 upon co-expression with F-AQP2-P262L (Fig. 5E) and appearance of G-AQP2 in the basolateral membrane (Fig. 5B) might be due to its interaction with F-AQP2-P262L, because with forskolin some AQP2-P262L was targeted to this domain. Thirdly, the 32 kDa band of F-AQP2-P262L, which seems indicative for its missorting, is absent upon co-expressing with G-AQP2, but not with G-AQP2-R187C (Fig. 5A).

Extrapolated to the NDI patients, the recessive inheritance of NDI in the studied families can be explained as follows: In the two patients, AQP2-R187C and AQP2-A190T mutants are retained in the ER, and do not interact with AQP2-P262L. AQP2-P262L is properly folded and assembles into homotetramers, but will be mainly retained in intracellular vesicles. The consequent lack of sufficient AQP2 proteins in the apical membrane of their collecting duct cells then explains their NDI phenotype. In the parents encoding wt-AQP2 and AQP2-R187C/A190T, wt-AQP2 will not interact with either mutant, but will form homotetrameric complexes, of which the insertion into the apical membrane in collecting duct cells will be properly regulated by vasopressin. Although the AQP2 expression levels in these humans might be reduced, because all AQP2 is derived from one allele, the apparent absence of an NDI phenotype indicates that AQP2 derived from one allele suffices for a healthy phenotype. In the proband's healthy relatives encoding wt-AQP2 and AQP2-P262L, both proteins are likely to assemble into heterotetramers. The dominancy of wt-AQP2 on the localization of AQP2-P262L will then result in a proper AVP-regulated trafficking of the wt-AQP2/AQP2-P262L complexes to the apical membrane of their collecting duct cells.

Molecular cause of the intracellular retention of AQP2-P262L

It is at present unclear which molecular mechanism is fundamental to the retention of AQP2-P262L. AQP2-P262A is, similar to wt-AQP2, re-distributed from intracellular vesicles to the apical membrane with forskolin (Fig. 4), which revealed that the introduced Leu instead of the lost Pro residue causes the missorting of AQP2-P262L.

Although the AQP2-P262L band with a 1 kDa increased mass could not always be discriminated from the smaller band because of the small difference in size, it seems indicative for its missorting. As AQP2-P262L is also expressed as a band with a size similar to that of unglycosylated wt-AQP2, the increased mass AQP2-P262L band might be due to a post-translational modification or a conformational instability induced by the P262L mutation. However, PNGaseF treatment of lysates of AQP2-P262L-expressing oocytes did not result in its disappearance, which indicated that its higher mass was not due to a modification at an N-glycosylation site (data not shown), and bio-informatical analysis revealed that the P262L mutation did not introduce or remove putative post-translational modification sites.

At present, it is also unclear whether the modification of AQP2-P262L is causing its missorting or is the result of its missorting. Interestingly, the ratio of 30 versus 29 kDa AQP2-P262L in plasma membranes of oocytes is inversely related to its expression levels. Similarly, with expression of different amounts of AQP2-R187C in oocytes, the ratio of high mannose glycosylated versus non-glycosylated forms was inversely related to its expression levels, which is thought to be a reflection of the level of retention of AQP2-R187C in the ER (27). The solution to these issues has to await detailed analysis of the location and identity of the modification.

In conclusion, we identified two families in which the recessive inheritance of NDI coincides with a P262L mutation that was located in a part of AQP2 that would have been anticipated to lead to dominant NDI. Detailed cell-biological analysis revealed that it indeed exerted most of the features of an AQP2 mutant in dominant NDI, but that, in contrast to mutants in dominant NDI, the apical sorting information in wt-AQP2 was dominant over the retention information in AQP2-P262L. As such, the AQP2-P262L mutant provides a unique and alternative cell-biological explanation for the occurrence of recessive NDI. Although it has been shown that recessive inheritance of diseases involving G-protein coupled receptors can have different cell-biological causes (e.g. misfolding, lack of agonist or G-protein binding), this has, to our recollection, never been reported for channels. Besides AQP2, it has been shown that misfolding of homotetrameric plasma membrane channels (e.g. ROMK1, KIR6.2, MIP26) underlies the recessive inheritance of other diseases (28,29). Possibly, missorting of the mutant and the rescue thereof by the wild-type protein also underlie the recessive nature of these diseases in some families.

MATERIALS AND METHODS

Analysis of patients

The proband in family A was evaluated clinically as previously described (30). Infusion of dDAVP was performed as described (0.3 μg/kg of body weight infused in 30 min) (31).

The *V2R* genes of the patients and their relatives were sequenced as described (32). The *AQP2* gene of the patients and their relatives was sequenced from genomic DNA as described (33). Genotyping of three loci (*AFM259vf9*, *D12S131*, *AFMb007yg5*) that flank the *AQP2* gene in chromosome region 12q13 was done to follow the segregation of the NDI allele in each family (34). *AFM259vf9*, *D12S131* and *AFMb007yg5* are dinucleotide repeats. A haplotype, which is the specific combination of alleles at closely linked loci, was assigned for these three loci. For our interpretation of the haplotype data, we assumed no recombination within an ~1.5 Mb region spanned by *AFM259vf9* and *AFMb007yg5*. Haplotype data provided support that the pedigree was consistent with stated biologic parentage.

Constructs

The oocyte expression constructs pT7Ts-AQP2 and pT7Ts-AQP2-R187C, AQP2-F and AQP2-R187C-F (here annotated as F-AQP2 and F-AQP2-R187C, because the tag was N-terminally fused) were as described (6,9,10,17). To facilitate cloning of mutant AQP2 cDNAs into the eukaryotic expression vector pCB6, the *Bam*HI site of pCB6 was removed by cutting the vector with *Bam*HI, blunting and religation to yield pCB6ΔBHI. To generate pCB6-ΔBHI-AQP2, a *Bgl*II/*Spe*I fragment of pT7Ts-AQP2 was isolated and cloned into the *Bgl*II/*Xba*I sites of pCB6ΔBHI. AQP2-P262L cDNA was obtained using the Altered Sites II *in vitro* mutagenesis kit (Promega, Madison, WI, USA) using a sense primer 5′-GCTGCACTCG**CTG**CAGAGCCTGC-3′ [mutation (bold) and introduced *Pst*I site (underlined) indicated] and its antisense counterpart on a pT7Ts-AQP2 template. After digestion with *Bam*HI and *Kpn*I, a 282 bp fragment was isolated and inserted into the corresponding sites of pT7Ts-AQP2 to generate pT7Ts-AQP2-P262L. pT7Ts-AQP2-A190T and pT7Ts-AQP2-P262A were constructed by three-point PCRs. For this, sense primers for AQP2-A190T (5′-GCCCGCTCCC TGACTCCGGCTGTCGTCACTGG-3′) and AQP2-P262A (5′-GCTGCACTCGGCCCAGAGCCTGC-3′) or the corresponding antisense primers were combined with a pT7Ts-AQP2 reverse primer (5′-GCGGCCCTCAGGCCTT GGTA-3′) and forward primer (5′- GCGAGAGCGAGTG CCCG-3′), respectively, in a standard PCR on a pT7Ts−AQP2 template. The resulting fragments were isolated, combined with each other and the flanking primers to generate the full-length mutated AQP2 fragments. Again, the *Bam*HI−*Kpn*I fragments were isolated and ligated into the corresponding sites of pT7Ts−AQP2 or pCB6-ΔBHI-AQP2 to generate pT7Ts-AQP2-A190T and pT7Ts-AQP2-P262A or pCB6-AQP2-P262A, respectively. To generate pCB7-AQP2 with a FLAG-tag (F; DYKDDDDK) at the N-terminus, pBS-F-AQP2 (17) was cut with *Not*I, blunted and digested with *Hin*dIII to cut out FLAG-tagged AQP2 (FLAG-AQP2). From pCB7, which is similar to pCB6, but contains a hygromycin instead of neomycin resistance cassette, the *Bam*HI site was removed by cutting, blunting and religation, generating pCB7ΔBHI. Then, the F-AQP2 fragment was ligated into the *Hin*dIII and blunted *Kpn*I site of pCB7ΔBHI to yield pCB7ΔBHI-F-AQP2. To generate pCB7-FLAG -AQP2-P262L (F-P262L), a 282 bp *Bam*HI−*Kpn*I fragment was isolated from pT7Ts-P262L and ligated into the corresponding sites of pCB7-FLAG-wt-AQP2ΔBHI. Introduction of only the desired mutations was confirmed by DNA sequence analysis.

Analyses in oocytes

Isolation and de-folliculation of *Xenopus laevis* oocytes, and isolation of total membranes or plasma membranes were performed as described (17,35). For transcription, the pT7Ts constructs were linearized with *Sal*I. Synthesis and purification of G-capped cRNAs and the subsequent analysis of their integrity and concentration were performed as described previously (17). Oocytes were (co-)injected with cRNAs and analyzed in a standard swelling assay at 2 or 3 days after injection (6).

Immunoprecipitation and immunoblotting

An aliquot of 15 μl of protein-G agarose beads per sample of solubilized total membranes of 25 oocytes was washed three times with 500 μl IPP500 [500 mM NaCl, 10 mM Tris (pH = 8.0), 0.1% NP-40, 0.1% Tween-20] plus protease inhibitors [1 mM PMSF, 5 μg/ml leupeptin and pepstatin A]. Subsequently, 3 μl of the FLAG-antibody (Sigma-Aldrich, The Netherlands) was added per sample and incubated overnight at 4°C. The solubilized total membranes were diluted with 600 μl of 10% sucrose and 100 mM NaCl, followed by incubation with antibody coupled agarose beads overnight at 4°C. Next, the beads were washed three times with IPP100 [100 mM NaCl, 10 mM Tris (pH = 8.0), 0.1% NP-40, 0.1% Tween 20] plus protease inhibitors, sucked dry with a 30 g needle and resuspended in 50 μl Laemmli.

Immunoblotting was performed as described (17). Blots were incubated with 1:3000 diluted affinity-purified rabbit anti-AQP2: 257–271, 1:20 000 diluted mouse anti-β-actin (AC15; Sigma, St Louis, MO, USA) or 1:5000 diluted rabbit anti-GFP antibodies (10,36). As secondary antibodies, a 1:5000 dilution of goat anti-rabbit IgGs (Sigma) coupled to horseradish peroxidase was used. For semi-quantification purposes, 2-fold dilution series of wt-AQP2 were blotted in parallel.

Culturing, transfection and immunocytochemistry of MDCK cells

MDCK cells stably expressing wt-AQP2 or GFP-tagged AQP2 (G-AQP2) have been described (9,18). MDCK cell culturing, stable cell transfection and selection of clones were done as described (37). Transient transfection was done with Lipofectamine 2000 reagent (Invitrogen, Breda, The Netherlands) according to manufacturer's protocol.

Immunocytochemistry and side-specific biotinylation

Two days after injection of cRNAs, vitelline membranes were removed from oocytes, after which they were fixed, paraffin embedded, sectioned and used for immunocytochemistry as described (17). Treatment with indomethacin and forskolin, and immunocytochemistry of polarized MDCK cells were done as described (37), except that blocking occurred for 20 min in phosphate-buffered saline (PBS) containing 0.1% bovine serum albumin, cells were permeabilized with 0.05% saponin in PBS and that antibody incubations were done for 30 min. As reported, indomethacin is an inhibitor of prostaglandin synthesis and reduces basal cAMP levels in MDCK-AQP2 cells (18). How prostaglandins increase the cAMP levels is unclear, but is thought to be due to paracrine activation of adenylyl cyclase-stimulating E-prostanoid $(EP)_2$ or EP_4 receptors. As primary antibodies, 1:100 dilutions of rat anti-E-Cadherin (DECMA, Sigma-Aldrich), rabbit anti-AQP2 antibodies, mouse anti-PDI (38) (kindly provided by D. Vaux, Oxford, UK) or FLAG antibodies (m2, Sigma-Aldrich) were used. As secondary antibodies, 1:100 diluted anti-rat, anti-rabbit or anti-mouse antibodies, conjugated to Alexa-488, Alexa-594 or Cy5 were used (Molecular Probes, Pitchford, Eugene, OR, USA). In cells co-expressing F-AQP2-P262L and wt-AQP2, F-AQP2-P262L was specifically detected with anti-FLAG-tag antibodies, whereas wt-AQP2 was detected with AQP2 antibodies, which, however, also binds F-AQP2-P262L. Therefore, to reveal only the signals for wt-AQP2, the signals obtained for F-AQP2-P262L with the FLAG antibodies were subtracted from the anti-AQP2 antibodies signals using Image Pro Plus 4.5 software (Media Cybernetics, Silver Spring, MD, USA). The subcellular localization of the different proteins was analyzed using a Bio-Rad CLSM with a 60× oil-immersion objective, a 32 Kalmann collection filter, an aperture diaphragm of 2.8 and an axial resolution of 0.4 μm per pixel. Side-specific biotinylation of MDCK cells was done as described (37).

Densitometrical analysis

To relate the plasma membrane expression of AQP2-P262L and wt-AQP2 in oocytes to their total expression, immunoblot signals were semi-quantified by measuring the integrated optical densities (IOD) on the films using the Image-Pro Plus analysis software (Media Cybernetics, Silver Springs, CO, USA). These signals were compared with the signals of a 2-fold dilution series of wt-AQP2, which was blotted in parallel. Background IOD values were determined at unexposed areas of the film and subtracted from obtained IOD values for the different proteins.

ACKNOWLEDGEMENTS

We thank Drs David Vaux (Oxford, UK) and Be Wieringa (Nijmegen, The Netherlands) for providing the PDI and GFP antibodies, respectively. This research was supported by grants from the Dutch Organization of Scientific Research (NWO-MW 902-18-292) to P.M.T.D. and P.v.d.S., and to E.J.K. (NWO; 916.36.122), from the European Union (QLRT-2000-00778; QLK3-CT-2001-00987) and kidney foundation (PC159) to P.M.T.D., from the Canadian Institutes of Health Research (MOP-8126) and the kidney foundation of Canada to D.G.B., and from the National Center for Research Resources, National Institutes of Health (M01 RR00048) to Feinberg Medical School of Northwestern University. We disclose all commercial affiliations/conflicts of interest.

REFERENCES

1. Deen, P.M.T. and Knoers, N.V.A.M. (1998) Physiology and pathophysiology of the aquaporin-2 water channel. *Curr. Opin. Nephrol. Hypertens.*, **7**, 37–42.
2. Nielsen, S., Kwon, T.H., Christensen, B.M., Promeneur, D., Frokiaer, J. and Marples, D. (1999) Physiology and pathophysiology of renal aquaporins. *J. Am. Soc. Nephrol.*, **10**, 647–663.
3. Nishimoto, G., Zelenina, M., Li, D., Yasui, M., Aperia, A., Nielsen, S. and Nairn, A.C. (1999) Arginine vasopressin stimulates phosphorylation of aquaporin-2 in rat renal tissue. *Am. J. Physiol.*, **276**, F254–F259.
4. Rosenthal, W., Seibold, A., Antaramian, A., Lonergan, M., Arthus, M.-F., Hendy, G.N., Birnbaumer, M. and Bichet, D.G. (1992) Molecular identification of the gene responsible for congenital nephrogenic diabetes insipidus. *Nature*, **359**, 233–235.
5. van den Ouweland, A.M., Dreesen, J.C., Verdijk, M.A.J. and Knoers, N.V.A.M. (1992) Mutations in the vasopressin type 2 receptor gene (AVPR2) associated with nephrogenic diabetes insipidus. *Nat. Genet.*, **2**, 99–102.
6. Deen, P.M.T., Verdijk, M.A.J., Knoers, N.V.A.M., Wieringa, B., Monnens, L.A.H., van Os, C.H. and van Oost, B.A. (1994) Requirement of human renal water channel aquaporin-2 for vasopressin-dependent concentration of urine. *Science*, **264**, 92–95.
7. van Lieburg, A.F., Verdijk, M.A.J., Knoers, N.V.A.M., van Essen, A.J., Proesmans, W., Mallmann, R., Monnens, L.A.H., van Oost, B.A., van Os, C.H. and Deen, P.M.T. (1994) Patients with autosomal nephrogenic diabetes insipidus homozygous for mutations in the aquaporin 2 water-channel gene. *Am. J. Hum. Genet.*, **55**, 648–652.
8. Mulders, S.M., Bichet, D.G., Rijss, J.P.L., Kamsteeg, E.J., Arthus, M.F., Lonergan, M., Fujiwara, M., Morgan, K., Leijendekker, R., van der Sluijs, P., van Os, C.H. and Deen, P.M.T. (1998) An aquaporin-2 water channel mutant which causes autosomal dominant nephrogenic diabetes insipidus is retained in the Golgi complex. *J. Clin. Invest.*, **102**, 57–66.
9. Marr, N., Bichet, D.G., Hoefs, S., Savelkoul, P.J., Konings, I.B., De Mattia, F., Graat, M.P., Arthus, M.F., Lonergan, M., Fujiwara, T.M. *et al.* (2002) Cell-biologic and functional analyses of five new aquaporin-2 missense mutations that cause recessive nephrogenic diabetes insipidus. *J. Am. Soc. Nephrol.*, **13**, 2267–2277.
10. Deen, P.M.T., Croes, H., van Aubel, R.A., Ginsel, L.A. and van Os, C.H. (1995) Water channels encoded by mutant aquaporin-2 genes in nephrogenic diabetes insipidus are impaired in their cellular routing. *J. Clin. Invest.*, **95**, 2291–2296.
11. Mulders, S.M., Knoers, N.V.A.M., van Lieburg, A.F., Monnens, L.A.H., Leumann, E., Wuhl, E., Schober, E., Rijss, J.P.L., van Os, C.H. and Deen, P.M.T. (1997) New mutations in the *AQP2* gene in nephrogenic diabetes insipidus resulting in functional but misrouted water channels. *J. Am. Soc. Nephrol.*, **8**, 242–248.
12. Murata, K., Mitsuoka, K., Hirai, T., Walz, T., Agre, P., Heymann, J.B., Engel, A. and Fujiyoshi, Y. (2000) Structural determinants of water permeation through aquaporin-1. *Nature*, **407**, 599–605.
13. Sui, H., Han, B.G., Lee, J.K., Walian, P. and Jap, B.K. (2001) Structural basis of water-specific transport through the AQP1 water channel. *Nature*, **414**, 872–878.
14. Marr, N., Bichet, D.G., Lonergan, M., Arthus, M.F., Jeck, N., Seyberth, H.W., Rosenthal, W., van Os, C.H., Oksche, A. and Deen, P.M.T. (2002) Heteroligomerization of an aquaporin-2 mutant with wild-type Aquaporin- 2 and their misrouting to late endosomes/lysosomes explains dominant nephrogenic diabetes insipidus. *Hum. Mol. Genet.*, **11**, 779–789.
15. Kuwahara, M., Iwai, K., Ooeda, T., Igarashi, T., Ogawa, E., Katsushima, Y., Shinbo, I., Uchida, S., Terada, Y. Arthus, M.F. *et al.* (2001) Three families with autosomal dominant nephrogenic diabetes insipidus caused by aquaporin-2 mutations in the C-terminus. *Am. J. Hum.Genet.*, **69**, 738–748.

16. Kamsteeg, E.J., Bichet, D.G., Konings, I.B., Nivet, H., Lonergan, M., Arthus, M.F., van Os, C.H. and Deen, P.M. (2003) Reversed polarized delivery of an aquaporin-2 mutant causes dominant nephrogenic diabetes insipidus. *J. Cell. Biol.*, **163**, 1099–1109.
17. Kamsteeg, E.J., Wormhoudt, T.A., Rijss, J.P.L., van Os, C.H. and Deen, P.M.T. (1999) An impaired routing of wild-type aquaporin-2 after tetramerization with an aquaporin-2 mutant explains dominant nephrogenic diabetes insipidus. *EMBO J.*, **18**, 2394–2400.
18. Deen, P.M.T., Rijss, J.P.L., Mulders, S.M., Errington, R.J., van Baal, J. and van Os, C.H. (1997) Aquaporin-2 transfection of Madin–Darby canine kidney cells reconstitutes vasopressin-regulated transcellular osmotic water transport. *J. Am. Soc. Nephrol.*, **8**, 1493–1501.
19. Deen, P.M.T., van Aubel, R.A., van Lieburg, A.F. and van Os, C.H. (1996) Urinary content of aquaporin 1 and 2 in nephrogenic diabetes insipidus. *J. Am. Soc. Nephrol.*, **7**, 836–841.
20. Tamarappoo, B.K. and Verkman, A.S. (1998) Defective aquaporin-2 trafficking in nephrogenic diabetes insipidus and correction by chemical chaperones. *J. Clin. Invest.*, **101**, 2257–2267.
21. Hirano, K., Zuber, C., Roth, J. and Ziak, M. (2003) The proteasome is involved in the degradation of different aquaporin-2 mutants causing nephrogenic diabetes insipidus. *Am. J. Pathol.*, **163**, 111–120.
22. Ward, C.L., Omura, S. and Kopito, R.R. (1995) Degradation of CFTR by the ubiquitin–proteasome pathway. *Cell*, **83**, 121–127.
23. Werner, E.D., Brodsky, J.L. and Mccracken, A.A. (1996) Proteasome-dependent endoplasmic reticulum-associated protein degradation: An unconventional route to a familiar fate. *Proc. Natl Acad. Sci. USA*, **93**, 13797–13801.
24. Kuwahara, M. (1998) Aquaporin-2, a vasopressin-sensitive water channel and nephrogenic diabetes insipidus. *Intern. Med.*, **37**, 215–217.
25. Shinbo, I., Fushimi, K., Kasahara, M., Yamauchi, K., Sasaki, S. and Marumo, F. (1999) Functional analysis of aquaporin-2 mutants associated with nephrogenic diabetes insipidus by yeast expression. *Am. J. Physiol.*, **277**, F734–F741.
26. Hendriks, G., Koudijs, M., van Balkom, B.W., Oorschot, V., Klumperman, J., Deen, P.M. and van der Sluijs, P. (2004) Glycosylation is important for cell surface expression of the water channel aquaporin-2 but is not essential for tetramerization in the endoplasmic reticulum. *J. Biol. Chem.*, **279**, 2975–2983.
27. Kamsteeg, E.J. and Deen, P.M.T. (2000) Importance of aquaporin-2 expression levels in genotype–phenotype studies in nephrogenic diabetes insipidus. *Am. J. Physiol. Renal Physiol.*, **279**, F778–F784.
28. Francis, P., Chung, J.J., Yasui, M., Berry, V., Moore, A., Wyatt, M.K., Wistow, G., Bhattacharya, S.S. and Agre, P. (2000) Functional impairment of lens aquaporin in two families with dominantly inherited cataracts. *Hum. Mol. Genet.*, **9**, 2329–2334.
29. Shieh, C.C., Coghlan, M., Sullivan, J.P. and Gopalakrishnan, M. (2000) Potassium channels: molecular defects, diseases, and therapeutic opportunities. *Pharmacol. Rev.*, **52**, 557–594.
30. Robertson, G.L. (2001) Antidiuretic hormone: normal and disorder function. *Endocr. Metab. clinics N. Am.*, **30**, 671–694.
31. Bichet, D.G., Razi, M., Lonergan, M., Arthus, M.-F., Papukna, V., Kortas, C. and Barjon, J.N. (1988) Hemodynamic and coagulation responses to 1-desamino [8-D-arginine] vasopressin in patients with congenital nephrogenic diabetes insipidus. *N. Engl. J. Med.*, **318**, 881–887.
32. Arthus, M.F., Lonergan, M., Crumley, M.J., Naumova, A.K., Morin, D., De Marco, L.A., Kaplan, B.S., Robertson, G.L., Sasaki, S., Morgan, K., Bichet, D.G. and Fujiwara, T.M. (2000) Report of 33 novel AVPR2 mutations and analysis of 117 families with X-linked nephrogenic diabetes insipidus [in process citation]. *J. Am. Soc. Nephrol.*, **11**, 1044–1054.
33. Lin, S.H., Bichet, D.G., Sasaki, S., Kuwahara, M., Arthus, M.F., Lonergan, M. and Lin, Y.F. (2002) Two novel aquaporin-2 mutations responsible for congenital nephrogenic diabetes insipidus in Chinese families. *J. Clin. Endocrinol. Metab.*, **87**, 2694–2700.
34. LeBlanc Straceski, J.M., Montgomery, K.T., Kissel, H., Murtaugh, L., Tsai, P., Ward, D.C., Krauter, K.S. and Kucherlapati, R. (1994) Twenty-one polymorphic markers from human chromosome 12 for integration of genetic and physical maps. *Genomics*, **19**, 341–349.
35. Kamsteeg, E.J. and Deen, P.M.T. (2001) Detection of aquaporin-2 in the plasma membranes of oocytes: a novel isolation method with improved yield and purity. *Biochem. Biophys. Res. Commun.*, **282**, 683–690.
36. Cuppen, E., van Ham, M., Wansink, D.G., de Leeuw, A., Wieringa, B. and Hendriks, W. (2000) The zyxin-related protein TRIP6 interacts with PDZ motifs in the adaptor protein RIL and the protein tyrosine phosphatase PTP-BL. *Eur. J. Cell Biol.*, **79**, 283–293.
37. Deen, P.M.T., Van Balkom, B.W.M., Savelkoul, P.J., Kamsteeg, E.J., Van Raak, M., Jennings, M.L., Muth, T.R., Rajendran, V. and Caplan, M.J. (2002) Aquaporin-2: COOH terminus is necessary but not sufficient for routing to the apical membrane. *Am. J. Physiol. Renal Physiol.*, **282**, F330–F340.
38. Fricker, M., Hollinshead, M., White, N. and Vaux, D. (1997) Interphase nuclei of many mammalian cell types contain deep, dynamic, tubular membrane-bound invaginations of the nuclear envelope. *J. Cell Biol.*, **136**, 531–544.